Published in final edited form as:
Ultrasound Med Biol. 2014 September ; 40(9): 2172–2182. doi:10.1016/j.ultrasmedbio.2014.03.018.

Non-contact high-frequency ultrasound microbeam stimulation for studying mechanotransduction in human umbilical vein endothelial cells

Jae Youn Hwang[1,†], **Hae Gyun Lim**[2], **Chi Woo Yoon**[2], **Kwok Ho Lam**[3], **Sangpil Yoon**[2], **Changyang Lee**[2], **Chi Tat Chiu**[2], **Bong Jin Kang**[2], **Hyung Ham Kim**[2], and **K. Kirk Shung**[2]

[1]Department of Information and Communication Engineering, Daegu Gyeongbuk Institute of Science & Technology, Daegu, Korea

[2]Department of Biomedical Engineering, University of Southern California, Los Angeles, CA 90089, USA

[3]Department of Electrical Engineering, Hong Kong Polytechnic University, Hunghom, Kowloon, Hong Kong

Abstract

In this paper, we demonstrate that contactless high-frequency ultrasound microbeam stimulation (HFUMS) is capable of eliciting cytoplasmic calcium (Ca^{2+}) elevation in human umbilical vein endothelial cells (HUVECs) and the associated mechanisms were highly correlated with those of shear force induced cytoplasmic Ca^{2+} elevation. Cellular mechanotransduction process which includes cell sensing and adaptation to mechanical microenvironment has been studied extensively in recent years. A variety of tools for mechanical stimulation has been developed to produce cellular response. We have developed a novel tool, highly focused ultrasound microbeam, for non-contact cell stimulation at a micro-scale. This tool at 200 MHz was applied to HUVECs to investigate its potential in eliciting cytoplasmic Ca^{2+} elevation. It was found that the response was dose-dependent and moreover extracellular Ca^{2+} and cytoplasmic Ca^{2+}stores were involved in the Ca^{2+} elevation. These results suggested that HFUMS may be potentially a novel non-contact tool for studying cellular mechanotransduction if the acoustic pressures at such high frequency could be quantified.

Keywords

high-frequency ultrasound microbeam; mechanotransduction; human umbilical vein endothelial cells; calcium fluorescence imaging

[†]Corresponding author: **Jae Youn Hwang, Ph. D.**, Department of Information and Communication Engineering, Daegu Gyeongbuk Institute of Science & Technology, Daegu, Korea, Address: 333 Techno Jungang-daero, Daegu, South Korea, 711-873, Tel: (+82) 53-785-6317, Fax: (+82) 53-785-6309, jyhwang@dgist.ac.kr.

Introduction

Cellular mechanotransduction represents the cellular processes that translate mechanical forces and deformations into biochemical signals such as activation of signaling pathway or changes in the cytoplasmic calcium level (Jaalouk and Lammerding 2009). For the past few decades, various molecular signaling pathways involved in cellular mechanotransduction have been extensively identified. For example, mechanotransduction signaling may be not only mediated by glycocalix in the response of endothelial cells to fluid shear stress (Pahakis et al. 2007), but also activated by force-induced unfolding of extracellular matrix proteins such as fibronectin (Sun et al. 2012). Also, it was found that cell-matrix focal adhesions are involved in the response of cells to their mechanical microenvironment (Geiger et al. 2009).

Mechanotransduction of vascular endothelial cells including human umbilical vein endothelial cells (HUVECs) may play an important role in maintaining homeostasis of vascular systems. The endothelial cells sensitively respond to external mechanical stimuli and correspondingly modify cytoplasmic signaling, gene expression, and protein expression (Chien 2007). Particularly, cytoplasmic Ca^{2+} concentration in HUVECs has been shown to have crucial roles in cellular mechanotransduction. The cytoplasmic Ca^{2+} elevations in endothelial cells, elicited in response to shear stress, triggered successive physiological and biochemical reactions including activation of Src tyrosine kinase and C kinase or production of nitric oxide and also resulted in the morphological changes and cell migration (Davies 1995; Yoshikawa et al. 1999). Moreover, the cytoplasmic Ca^{2+} elevation was involved in actomyosin contractility in HUVECs (Feneberg et al. 2004). Various important roles of Ca^{2+} have been so far identified in the cell mechanotransduction. However, it still remains unclear how the cells sense mechanical forces and trigger cytoplasmic molecular signals.

In the cell mechanotransduction study, well-defined mechanical stimulation to a cell is also highly important in identifying molecular signaling pathways in response to the exerted stimulus. Therefore, various tools have been developed to allow the quantitative analysis of effects of mechanical forces on cellular mechanotransduction. For example, a mechanical stimulation device, in which elastic gels where cells were cultured were mechanically vibrated, enabled localized mechanical stimulation of cells at subcellular levels (Nishitani et al. 2011). A flow chamber, which enabled sudden expansion in the diameter of the chamber, allowed discrimination between the effects of temporal gradients and spatial gradients in shear stress on extracellular signal-regulated kinases 1 and 2 activation (Jiang et al. 2002). Optical tweezers offered focal and prolonged stimulation of neurons by pulling a trapped microbead attached to a cell (D'Este et al. 2011).

Cellular responses at low-frequency ultrasound have been examined for a variety of cells. It was found that the low frequency ultrasound could elicit changes in calcium levels in cells. For example, osteoblastic cells exhibited calcium elevations upon the application of 3.5 MHz ultrasound (Zhang et al. 2012). Also, 1 MHz ultrasound elicited calcium influx into Chinese hamster ovary cells in the presence of albumin-encapsulated Optison microbubbles (Kumon et al. 2007). In addition, ultrasound stimulation of cells could modulate signal transduction pathways (Whitney et al. 2012), cytoskeletal organization (Noriega et al. 2013), and neuronal development (Hu et al. 2013). In particular, low intensity continuous

ultrasound stimulation of chondrocytes induced the expression of chondrogenic markers such as Sox-9 and type II collagen (Noriega et al. 2007; Hasanova et al. 2011) as well as phosphorylation of focal adhesion kinase, src, etc (Whitney et al. 2012). Furthermore, the low-frequency ultrasound affected nuclear processes of the cells including the expression of early response gens c-Fos, c-Jun, and c-Myc while the magnitude of effect depended on the ultrasound frequency (Louw et al. 2013). In contrast, we recently demonstrated that high-frequency ultrasound microbeam was better suited for more localized single-cell stimulation (Hwang et al. 2012; Hwang et al. 2013) than the low-frequency ultrasound. Particularly, high-frequency ultrasound microbeam stimulation (HFUMS) allowed identifying functional characteristics of cells and also discriminating cell types (Hwang et al. 2012; Hwang et al. 2013). In these studies, it was found that HFUMS resulted in more reduction of mitochondrial membrane potentials in breast cancer cells than in normal cells, thus showing its capability to discriminate between the functional characteristics of the cells (Hwang et al. 2012; Hwang et al. 2013). In addition, it was observed that the HFUMS elicited different levels of cytoplasmic calcium (Ca^{2+}) elevations in highly and weakly invasive breast cancer cells (Hwang et al. 2012; Hwang et al. 2013).

In this paper, we report results from an investigation into whether contactless 200 MHz high-frequency ultrasound microbeam stimulation (HFUMS) is capable of eliciting calcium signaling responses of HUVECs, demonstrating the potential of HFUMS as a cell stimulator for cellular mechanotransduction studies. Cytoplasmic calcium changes in HUVECs were analyzed in response to HFUMS by using a fluorescent calcium indicator, membrane-permeant Fluo-4 AM. The dose-response relationship was obtained by varying the acoustic power including duty cycles of the input ultrasound signal. Finally, we investigated the dependence of HFUMS-induced cytoplasmic calcium elevations on extracellular calcium and cytoplasmic calcium stores, respectively.

Materials and Methods

Cell preparation and materials

Human umbilical vein endothelial cell lines were obtained from Cell Applications Inc. (San Diego, CA, USA) and maintained in endothelial cell growth medium. A calcium indicator, Fluo-4 AM was purchased from Invitrogen (Grand Island, NY, USA) for live-cell calcium fluorescence imaging. Gadolinium chloride, Thapsigargin, EDTA, and U73122 were purchased from Sigma-Aldrich (St. Louis, MO, USA) to investigate the dependences of HFUMS-induced Ca^{2+} elevation on extracellular calcium and cytoplasmic calcium stores in HUVECs. Rodamine B was purchased from Sigma-Aldrich to examine the temperature changes of media by HFUM application.

Mechanotransduction system for HFUMS and live-cell fluorescence imaging

In order to perform live-cell fluorescence imaging of HUVECs stimulated by HFUM, we used an experimental mechanotransduction system consisting of a high-frequency ultrasound microbeam generator (a tightly focused ultrasonic transducer), an inverted epi-fluorescence microscope (IX71, Olympus, Tokyo, Japan) (Fig 1.a) as demonstrated previously (Hwang et al. 2013). A press-focused ultra-high frequency single element lithium

niobate ($LiNbO_3$) transducer was constructed with conventional transducer fabrication procedures (Lam et al. 2012) to generate a highly focused ultrasound beam for single cell stimulation. The focal length and aperture diameter of the transducer were 0.75 mm and 0.65 mm, respectively (f-number=1.15). Note that the lower f-number of a transducer offered the narrower beam, thus producing more shear force than the transducer previously utilized (Hwang et al. 2012; Hwang et al. 2013). The center frequency was found to be 193 MHz (Fig. 1.b). The measured beam width of a highly focused ultrasound microbeam at focus was 9.0 μm (Fig 1.c, left). The depth of focus was estimated to be 65.9 μm (Fig 1.c, right). In order to generate a highly focused ultrasound microbeam, 200 MHz sinusoidal bursts from a function generator (SG384, STANFORD RESEARCH SYSTEMS, Sunnyvale, CA, USA) was amplified by a 50-dB power amplifier (525LA, ENI, Rochester, NY, USA), and the amplified bursts were directed to the transducer. The peak-to-peak (V_{pp}) voltages of the input bursts were adjusted to 9.48, 12.64, 15.80, and 18.96 V_{pp}. The duty cycles were tuned to 0.1, 0.25, 0.5, 0.75, and 1 %, and the pulse repetition frequency (PRF) was 1 kHz.

Using the epi-fluorescence microscope, live-cell fluorescence imaging was carried out to monitor cytoplasmic Ca^{2+} elevations in HUVECs elicited by HFUMS. Light from a mercury lamp was delivered to cells for excitation of calcium indicators loaded into the cells after passing through an electronic shutter, an excitation bandpass filter (488 nm±20 nm), a dichroic mirror (cut-off wavelength: 500 nm), and a 20× objective. Fluorescence emitted from the cells was collected by the same objective and then recorded using a high-sensitivity CCD camera (ORCA-Flash2.8, Hamamatsu, Middlesex, NJ, USA).

Precise localization of ultrasound microbeam focus on target cells

It is highly important to precisely focus the microbeam on a targeted cell to result in a response from the stimulated HUVECs. In our previous study, for precise focusing of the beam on a target cell, echoes were acquired while a transducer was scanned across a 6 μm tungsten wire target in the x- and y-direction (Hwang et al. 2013). The focal point was placed at the center of an image. In this study, we employed an acoustic trapping technique to localize the beam focus on a target cell. After a 5 μm microbead was trapped at the beam focus of the transducer, the 5 μm microbead was positioned at the center of an image. Note that the microbead was trapped in the acoustic beam center at focus, and therefore the location of the trapped microbead actually represented the location of the acoustic beam focus. Fig. 1.d illustrates the trapped microbead located at the center of the image field of view.

Live-cell calcium fluorescence imaging and quantitative analysis for cytoplasmic Ca^{2+} elevations in HUVECs

Fluo 4-AM was utilized for live-cell calcium fluorescence imaging. 10^5 cells were plated on 35 mm petri-dishes and incubated in the cell culture medium at 37 °C for 36 hours. After 1 μM Fluo 4-AM solution was added to the dishes, the cells were incubated at room temperature for 30 minutes and then washed with PBS. The target cell was positioned at the microbeam focus (the center of an image), followed by time-lapse fluorescence imaging of the cells. Fluorescence images were here acquired every 2 seconds for t = 300 seconds

(exposure time: 500 ms), as the HFUM was switched on and off at t = 60 seconds and t = 240 seconds, respectively.

Quantitative analysis of Ca^{2+} changes in HUVECs were performed using the program described previously (Hwang et al. 2013). The program provided a Cell Response Index (CRI) value, which indicates the degree of calcium response of cells to HFUMS. The CRI was calculated by multiplying the mean of normalized maximum calcium elevations and the cell responding ratio, which is the number of responding cells over the total number of cells (Hwang et al. 2013). Here a larger CRI indicated a stronger response to HFUMS. The CRIs of HUVECs under the indicated conditions were compared.

Reagents and inhibitor treatment

To examine dependence of HFUMS-induced cytoplasmic calcium elevations on calcium influx across the plasma membrane, two approaches including eliminating extracellular calcium and blocking stretch-activated ion channels in cell membrane were applied (Nishitani et al. 2011) : 1) EDTA at 5 mM was applied to cell culture media for 30 minutes to eliminate extracellular calcium in the media and 2) HUVECs were treated with Gadolinium (III) chloride at 3 μM for 20 minutes to block the stretch-activated ion channels. In addition, we examined the dependence of HFUMS-induced cytoplasmic calcium elevations on both endoplasmic reticulum and phospholipase C (PLC). HUVECs were treated with Thapsigargin at 1 μM for 45 minutes to inhibit endoplasmic reticulum calcium pump and deplete the cytoplasmic calcium stores, whereas U73122, PLC inhibitor, was applied to the cells at 5 μM for 10 minutes to block the release of inositol trisphosphate (IP3).

Cell Viability Test

After application of HFUMS to HUVECs, a cell viability test was performed with Calcein AM (Invitrogen, Grand Island, NY, USA), fluorescence viability indicators (Knight et al. 2003). For loading of the indicators into cells cultured in a petri-dish, the cells had been incubated in HBSS containing 1 μM Calcien at room temperature for 30 minutes and then were thoroughly washed with HBSS. After the petri-dish was placed on a microscope, fluorescence imaging of cells was performed before and after HFUMS (input voltage: 18.96 V_{pp}, duty factor: 0.5 %, PRF: 1 kHz, and exposure time: 180 seconds). In addition, the viability changes in the cells were compared with the cells treated with 10% bleach (control) at the indicated time points (5, 10, 15, and 20 minutes). Furthermore, we examined the cell viability at 1 hour and 24 hours after HFUMS with a LIVE/DEAD viability/cytotoxicity kit in which membrane-permeant Calcein AM yields cytoplasmic green fluorescence in live cells while membrane-impermeant ethidium homodimer-1 yields red fluorescence in nucleic acids of dead cells (Invitrogen, Grand Island, NY, USA). The microscope and transducer were decontaminated with 70% ethanol before carrying out the 24h long-term monitoring of cell viability. Also, two alcohol lamps were placed in front and at the back of a cell chamber, thus enabling to avoid cell contamination from multiple directions under the circumstances while performing the experiment. After HFUMS, the media in the cell chamber were replaced with fresh media and incubated at 37 °C for 24 hours, followed by the viability/cytotoxicity assay test. It is very difficult to find the same cells exposed to

HFUM in 24 hours due to their movement and morphological changes. As a result, a mark was placed on the bottom of the chamber with a black pen to find the same cells receiving HFUM prior to 24 hours,

Comsol simulation for estimation of acoustic pressures at focus

The acoustic pressure at the transducer's focal point was estimated by simulating the wave propagation using COMSOL Multiphysics (COMSOL Inc., Burlington, MA, USA). The simulation was considered as 2D axisymmetric. The geometry of the transducer for the simulation had three domains: (1) parylene matching layer with thickness of 2 m and acoustic impedance of 2.8 MRayls, (2) the lithium niobate crystal with thickness of 10 m and acoustic impedance of 18.8 MRayls, and (3) e-solder with the acoustic impedance of 5.5 MRalys. The focal point of a transducer was located at the surface of the petri-dish. The surrounding medium was water. During the simulation, four input voltages (9.48, 12.64, 15.8, and 18.96 V_{pp}) were applied to the lithium niobate crystal while the other side of the crystal was grounded. Duty cycle was kept 0.5 % with pulse repetition frequency of 1 kHz. At least 7 elements per wavelength were assigned to resolve the wavelength. The total number of elements and the degrees of freedom were 905474 and 2192390, respectively.

Monitoring changes in temperature of media by HFUMS

100 μM Rhodamine B solution diluted with carbonate buffer, in which its fluorescence intensity changes represent surrounding temperature changes, were utilized to examine the temperature changes at focus of HFUMS (Ross et al. 2001). Rhodamine B fluorescence images were acquired every 10 seconds for t = 300 seconds, as the HFUM was switched on and off at t = 60 seconds and t = 240 seconds, respectively to monitor temperature changes by HFUM application. Before monitoring the temperature changes by the HFUM application, we quantified fluorescence intensities of Rhodmaine B solution as a function of temperature in order to calibrate the fluorescence intensity. Fluorescence images of 100 μM Rhodamine B solution was acquired at different temperatures of 25, 27, 29, 31, 33, 35, and 37 °C and their fluorescence intensities at beam focus were measured. The temperature of Rhodmine B solution was here adjusted with a delta T chamber, which is a temperature-controlled chamber (Biotechs Inc. Butler, PA, USA).

Statistical Analysis

All data were expressed as mean ± standard deviation of indicated sample sizes, and were analyzed by a two-tailed paired *t*-test, with the level of significance set at $p\text{-value} < 0.05$. The number of cells was quantitated from over triplicate experiments.

Results

Cytoplasmic Ca^{2+} variations in HUVECs elicited by HFUMS

Live-cell fluorescence imaging was performed to monitor Ca^{2+} changes in HUVECs, stained with Fluo-4 AM, due to HFUMS. It was observed that HFUMS elicited significant fluorescence increases in HUVECs (Fig. 2.a) (Supplementary video 1 and Supplementary video 2). Fig. 2.b illustrates the normalized Ca^{2+} temporal variations in HUVECs due to HFUMS. The HUVECs clearly exhibited transient Ca^{2+} elevations when HFUM was on and

then the Ca^{2+} level in HUVECs was gradually reduced by ~ 1.25 at 240 s. In addition, the calcium elevations were further quantitated using the program described previously for the quantitative analysis. The CRI value for HUVECs stimulated by HFUM was ~1.89 whereas the CRI value for control cells (without HFUMS) was 0 (n=21) (Fig. 2.c). Therefore, these results clearly demonstrated that HFUMS elicited significant Ca^{2+} elevations in HUVECs compared to the control cells.

Effect of HFUM exposure on cytoplasmic Ca^{2+} elevation in HUVECs

Dependences of HFMUS-elicited cytoplasmic Ca^{2+} elevation on both input voltage to the transducer and duty cycle of the input bursts were examined. Note that acoustic pressure generated from the transducer is proportional to the input voltages to the transducer if the input power level is low (Johns et al. 2007). Fig. 3.a demonstrates the CRIs for HUVECs at the simulated acoustic power at the given input voltages. When the simulated acoustic pressure was 1.8 and 2.4 MPa, the normalized CRI values slightly increased up to 0.18 and 0.36 from the base-line (acoustic pressure = 0 MPa), respectively. In contrast, the CRI values at the simulated acoustic pressure of 3.0 and 3.6 MPa significantly increased up to almost three-fold over the CRI value at the simulated acoustic pressure of 2.4 MPa (*p*-value = 0.028 < 0.05). In this experiment, the CRI for HUVECs was highest when the simulated acoustic pressure was 3.6 MPa. In addition, we examined the dependence of calcium response of the cells to HFUMS on the duty cycle of input bursts. We here examined the CRI values for HUVECs at the lower duty cycles than 1 % (simulated acoustic pressure of 3.6 MPa) since few cells were detached from the cell culture dish by HFUMS at the simulated acoustic pressure of 3.6 MPa and the duty cycle of 1%.

The CRI values for HUVECs increased as a function of duty cycles as shown in Fig. 3.b. When the duty cycle was 0.10 % at 3.6 MPa, HUVECs did not exhibit any notable Ca^{2+} elevation. In contrast, the mean of CRI increased as the duty cycles further increased. The normalized CRI values at the duty cycles of 0.25 and 0.50 % were measured to be 0.41 and 0.78, respectively. Altogether, these results demonstrated that there was indeed a dose-response relationship between the CRI values and acoustic pressure in HUVECs.

Effects of extracellular calcium on HFUMS-induced Ca^{2+} elevations in HUVECs

Previous studies showed that upon mechanical stimulation of HUVECs, HUVECs exhibited cytoplasmic Ca^{2+} elevations. It is however important to note that the cytoplasmic Ca^{2+} elevations were affected by both extracellular calcium influx and Ca^{2+} release from cytoplasmic calcium stores (Yamamoto et al. 2000; Nishitani et al. 2011). To determine the origin of cellular Ca elevation, we first examined whether the extracellular Ca^{2+} effects on HFUMS-induced Ca^{2+} elevation in HUVECs. Both the calcium chelation of EDTA and $GdCl_3$ significantly inhibited calcium elevations in HUVECs (Fig. 4) due to HFUMS compared to those in the control cells (Fig. 2.a). The spontaneous calcium increases as shown in the untreated cells were not observed in the majority of the cells treated with EDTA and Gadolinium (III) chloride. The CRI values for HUVECs treated with the inhibitors were interestingly found to be 0. Therefore, these results suggested that the HFUMS-induced Ca^{2+} elevations in HUVECs were significantly affected by both extracellular calcium concentration and stretched-activated ion channels on cell membrane.

Effects of cytoplasmic calcium stores on HFUMS-induced Ca^{2+} elevations in HUVECs

We further examined the effects of cytoplasmic calcium stores, particularly endoplasmic reticulum (ER), and PLC on HFUMS-induced Ca^{2+} elevations in HUVECs. The ER blockers, Thapsigargin, significantly reduced HFUMS-induced Ca^{2+} elevations in HUVECs (Fig. 5) compared to those in the untreated cells (Fig. 2), thus showing that ER was highly involved in the Ca^{2+} elevations in HUVECs due to HFUMS. In addition, the PLC inhibitors, U73122, also reduced the Ca^{2+} elevations in HUVECs as shown in Fig. 5 compared to the control cells. The normalized mean maximum fluorescence of the responding cells (n=3) treated with ER blockers was 2.26±1.15 (CRI=0.61), whereas that of the responding cells (n=10) treated with PLC inhibitors was 1.28±0.21 (CRI=1.17). These results suggested that the HFUMS-induced Ca^{2+} elevations in HUVECs were significantly affected by the cytoplasmic calcium stores as well.

Effects of HFUMS on viability of HUVECs

We assessed HFUMS effects on the viability of HUVECs. Here we applied the same dosage of HFUMS used in the previous section. Fig. 6.a demonstrates the viability changes of HUVECs due to HFUMS at the indicated time-points. We here observed that the Calcien fluorescence in HUVECs was not significant changed due to HFUMS (Fig. 6.a and b) (*p*-value= 0.65 > 0.05) compared to the control (before stimulation) whereas the 10% bleach significantly reduced the viability of the cells at 5 minutes after initiation of the treatment. The mean fluorescence of the 10% bleach treated cells at 20 minutes decreased by 6.8 % over the mean florescence at 0 s (p-value=$4.9 \times 10^{-18} < 0.05$). In contrast, we observed that the majority of HUVECs exposed to HFUMS still maintained good viability at 20 minutes after exposure to HFUMS. Furthermore, we confirmed the cell viability in 1 hour and 24 hours after exposure to HFUMS using the LIVE/DEAD viability/cytotoxicity kit, respectively (Fig. 6.b and c). Figure 6.b and c demonstrated that all the cells receiving HFUM exhibited good viability which is indicated by green color (Fig. 6.b and c). In Fig. 6.c, the cells within the dotted-red rectangular received HFUM. In 24 hours, the cells still maintained their viability. Note that the red colored cells shown in Fig. 6.b and c seemed to be the fragmented cells, not receiving HFUMS. These results suggested that HFUMS did not affect the viability of HUVECs at the given acoustic pressure.

Discussion

This work demonstrates that HFUMS is capable of eliciting cytoplasmic calcium elevations in HUVECs in a non-contact manner. It was observed that the initiating times of transient Ca^{2+} elevations elicited by HFUMS differed slightly depending on the individual cells. Also, after the Ca^{2+} elevation by HFUMS, the intracellular Ca^{2+} levels in HUVECs were gradually decreased by the base-line with varying time courses. The previous studies showed that endothelial cells exhibited heterogeneous natures since they are significantly affected by the local environments, especially the interaction with surrounding cells (Garlanda and Dejana 1997; Mason et al. 1997). Here the heterogeneous responses of HUVECs to HFUMS might also result from the cells' heterogeneity.

Previous studies have shown that various types of mechanical stimulation can induce cytoplasmic calcium elevations in HUVECs. Mechanical vibration on HUVECs resulted in global calcium elevation (Nishitani et al. 2011). Shear stress was also observed to elicit cytoplasmic calcium elevation in the cells (Yoshikawa et al. 1999; Yamamoto et al. 2000). Radiation force is produced when ultrasound propagated in a medium. Therefore, it is likely that the cytoplasmic calcium elevations are caused by the mechanical stresses exerted by high-frequency ultrasound on the cell. In this study, we utilized the ultrahigh frequency transducer at 200 MHz with the f-number of ~ 1.15 in order to generate a highly-focused ultrasound microbeam at focus and therefore the lateral acoustic microbeam size of ~ 9 μm, which was smaller than those of the cultured HUVECs, could be achieved. Explicitly, strain force generated by tightly focused acoustic beams may be dominant at the center of an acoustic microbeam at focus compared to shear force, whereas the shear force by the acoustic beam may become dominant at the farther distance from the beam center compared to the strain force. Note that the more tightly-focused acoustic microbeam with smaller sizes generates the stronger shear force at focus (Lee et al. 2010). Hence, the smaller size of the acoustic beams may be beneficial to define the force type generated from the focused acoustic beams over the cells. For example, when the size of a tightly-focused acoustic beam becomes much smaller than the size of cells, the effects of strain force on the cells may be ignored compared to the effects of shear force on the cells. Therefore, in order to better define the type of acoustic forces applied on cells, it would be needed to make more high-frequency ultrasound transducers with lower f-number since the size of acoustic beams is dependent on the operating frequency of a transducer the f-number of the transducer, thus offering better definition of the mechanoenvironment.

The calcium response of HUVECs to HFUMS depended on the input voltage driving the transducer and the duty cycle of the input bursts (Fig. 3). Since the acoustic pressure at the focus is proportional to the input voltage to a transducer if the voltage level is low, these results indicate that the calcium response to HFUMS is related to the acoustic pressure exerted on the cell. The calcium response of HUVECs to HFUMS also increased proportionally as a function of duty cycle, thus indicating that the calcium response was related to the spatial peak temporal average intensity of ultrasound beams, which is proportional to the duty cycle. Currently, there are no devices capable of quantifying acoustic pressures of a transducer at such a high frequency (over ~ 100 MHz). Therefore, it is not possible to quantify the acoustic pressure at the focus. Hence, we have performed finite element analysis using commercial software to estimate acoustic pressure field of 200MHz transducer. The simulated results showed that the peak acoustic pressure linearly increased as the input voltage changed from 9.48 V_{pp} to 18.96 V_{pp} (supplementary Fig.1). In particular, the peak pressure at the input voltage of 18.96 V_{pp} (duty cycle: 0.5 %), which was used for the experiment on the dependences of HFUMS induced calcium elevation on extracellular calcium and intracellular calcium stores, was surprisingly found to be ~3.6 MPa at focus. Note that the absolute peak pressures were obtained under ideal conditions using COMSOL simulation. Therefore, the real acoustic pressure may be less than the simulated acoustic pressure. For better mechanotransduction study with HFUMS, these results must be validated with experimental data, and thus the development of a new method capable of quantifying the acoustic pressures at such high frequencies should be explored.

Although the stimulated acoustic pressure was surprisingly high, we could not observe any significant effect of HFUM on the cell viability due to probably the following reasons: 1) any significant temperature increase was not observed due to the applied HFUM as shown in Fig. 7. The temperature variations due to HFUM were less than 1 °C. These variations were also observed in the control experiment (Fig. 7.b) ; 2) the actual power delivered to the cell might be a lower level since the acoustic beam area was around ~ 6.35×10^{-9} cm^2; 3) typically, the peak negative pressure of 3 MPa at 500 kHz significantly reduced cell viability due to cavitation effect (Guzmán et al. 2001). However, even though the simulated acoustic pressure level was ~ 3.6 MPa, we here utilized ultra-high frequency (200 MHz). Therefore, the mechanical index (MI = peak negative pressure $(MPa) / \sqrt{\text{center frequency}}$) was calculated to be 0.2546. Note that the mechanical index is much less than the maximal allowable MI of 1.9 (Shung 2006).

In other previous studies, mechanical vibration and shear stress can elicit cytoplasmic Ca^{2+} elevations in HUVECs (Tanaami et al. 2002; Nishitani et al. 2011). However, it was found that the cytoplasmic Ca^{2+} elevations due to the external forces were significantly reduced by stretched-activated calcium channel blockers and the chelation of extracellular Ca^{2+} ions. Our results are in agreement with these observations (Fig. 4). Interestingly, although few EDTA-treated cells exhibited the slight Ca^{2+} elevations (Fig. 4), the CRI value for the cells was found to be 0. It may be caused by the slow cytoplasmic Ca^{2+} increases. Note that the program used for quantitative analysis of Ca^{2+} response was built to preferentially detect spontaneous Ca^{2+} elevations in a cell (Hwang et al. 2013).

In the Ca^{2+} response of HUVECs to external mechanical stimuli, it was also found that the PLC/IP3 pathway and the ER calcium release were crucial. Therefore, the PLC inhibitors and ER blockers reduced the Ca^{2+} response in HUVECs to the mechanical stimuli. Our work also confirms these findings (Fig. 5). It has been postulated that mechanical stimulation opens membrane channels in HUVECs and then induces Ca^{2+} influx across the cell membrane. The cytoplasmic Ca^{2+} increases due to the Ca^{2+} influx activates PLC-δ and triggers the IP3 signaling pathway. The IP3 release further induces another Ca^{2+} release from ER, yielding a global cytoplasmic Ca^{2+} elevation in HUVECs (Nishitani et al. 2011). In the aforementioned studies related to the dependence of HFUMS-induced calcium elevation in HUVECs on the extra calcium and intracalcium stores, the exposure time of HFUM to the cell was reduced by 60 seconds since we could observe that the most of calcium elevation was occurred within the initial period of HFUMS in the study related to the dependence of HFUMS induced calcium elevation in HUVECs on acoustic intensity.

Conclusions

This paper demonstrates that HFUMS is capable of eliciting cellular cytoplasmic Ca^{2+} increases in HUVECs without any direct contact. The Ca^{2+} response of HUVECs to the HFUMS was found to be dependent on both the peak-to-peak voltage applied to the transducer and the duty cycle of the applied signal, suggesting that there is a dose-response relationship. Furthermore, it was found that the HFUMS-elicited cytoplasmic Ca^{2+} elevation in HUVECs was related to both calcium influx through the stretch-gated ion channels and the calcium release from calcium stores, endoplasmic reticulum, showing the mechanistic

similarity to the results obtained by using other mechanical stimulation tools. Here it is importantly to note that HFUMS may have a few advantages over other stimulation methods including a microfluidic device (Liu et al. 2013), optical tweezers (Hayakawa et al. 2008), and glass probes (Hamilton et al. 2008). For example, HFUMS is non-contact and allows single cell stimulation at a micro scale (< ~9 m), which depends on ultrasound frequency. It can offer more versatility in stimulation of HUVECs in terms of beam size, intensity level, and force type.

Our previous studies mainly demonstrated the potentials of HFUMS for determination of invasion potential of breast cancer cells (Hwang et al. 2012; Hwang et al. 2013). In contrast, in this study, we found that HFUMS elicited calcium elevation in HUVECs and moreover the cellular mechanisms associated to the calcium elevation in HUVECs due to HFUMS were highly correlated with the previous findings, thus demonstrating the usefulness of HFUMS in the mechanotransduction study of HUVECs. However, for a better mechanotransduction study with HFUMS, force calibration of the transducer at such a high frequency of ~ 193 MHz should be carried out. This will be pursued vigorously in the future. If the force calibration of transducers at such the frequency is made possible, HFUMS may become an extremely useful stimulation tool for endothelial cell mechanotransduction study.

Supplementary Material

Refer to Web version on PubMed Central for supplementary material.

Acknowledgments

This work has been supported by the NIH grants (R01-EB012058 and P41-EB002182) to K.K. Shung.

References

Chien S. Mechanotransduction and endothelial cell homeostasis: the wisdom of the cell. Am J Physiol Heart Circ Physiol. 2007; 292:H1209–24. [PubMed: 17098825]

D'Este E, Baj G, Beuzer P, Ferrari E, Pinato G, Tongiorgi E, Cojoc D. Use of optical tweezers technology for long-term, focal stimulation of specific subcellular neuronal compartments. Integr Biol (Camb). 2011; 3:568–77. [PubMed: 21437309]

Davies PF. Flow-mediated endothelial mechanotransduction. Physiol Rev. 1995; 75:519–60. [PubMed: 7624393]

Feneberg W, Aepfelbacher M, Sackmann E. Microviscoelasticity of the apical cell surface of human umbilical vein endothelial cells (HUVEC) within confluent monolayers. Biophys J. 2004; 87:1338–50. [PubMed: 15298936]

Garlanda C, Dejana E. Heterogeneity of endothelial cells. Specific markers. Arterioscler Thromb Vasc Biol. 1997; 17:1193–202. [PubMed: 9261246]

Geiger B, Spatz JP, Bershadsky AD. Environmental sensing through focal adhesions. Nat Rev Mol Cell Biol. 2009; 10:21–33. [PubMed: 19197329]

Guzmán HR, Nguyen DX, Khan S, Prausnitz MR. Ultrasound-mediated disruption of cell membranes. I. Quantification of molecular uptake and cell viability. J Acoust Soc Am. 2001; 110:588–96. [PubMed: 11508983]

Hamilton N, Vayro S, Kirchhoff F, Verkhratsky A, Robbins J, Gorecki DC, Butt AM. Mechanisms of ATP- and glutamate-mediated calcium signaling in white matter astrocytes. Glia. 2008; 56:734–49. [PubMed: 18293404]

Hasanova GI, Noriega SE, Mamedov TG, Guha Thakurta S, Turner JA, Subramanian A. The effect of ultrasound stimulation on the gene and protein expression of chondrocytes seeded in chitosan scaffolds. J Tissue Eng Regen Med. 2011; 5:815–22. [PubMed: 22002925]

Hayakawa K, Tatsumi H, Sokabe M. Actin stress fibers transmit and focus force to activate mechanosensitive channels. J Cell Sci. 2008; 121:496–503. [PubMed: 18230647]

Hu Y, Zhong W, Wan JM, Yu AC. Ultrasound can modulate neuronal development: impact on neurite growth and cell body morphology. Ultrasound Med Biol. 2013; 39:915–25. [PubMed: 23415289]

Hwang JY, Lee J, Lee C, Jakob A, Lemor R, Medina-Kauwe LK, Kirk Shung K. Fluorescence response of human HER2+ cancer- and MCF-12F normal cells to 200MHz ultrasound microbeam stimulation: A preliminary study of membrane permeability variation. Ultrasonics. 2012; 52:803–8. [PubMed: 22513260]

Hwang JY, Lee NS, Lee C, Lam KH, Kim HH, Woo J, Lin MY, Kisler K, Choi H, Zhou Q, Chow RH, Shung KK. Investigating contactless high frequency ultrasound microbeam stimulation for determination of invasion potential of breast cancer cells. Biotechnol Bioeng. 2013

Jaalouk DE, Lammerding J. Mechanotransduction gone awry. Nat Rev Mol Cell Biol. 2009; 10:63–73. [PubMed: 19197333]

Jiang GL, White CR, Stevens HY, Frangos JA. Temporal gradients in shear stimulate osteoblastic proliferation via ERK1/2 and retinoblastoma protein. Am J Physiol Endocrinol Metab. 2002; 283:E383–9. [PubMed: 12110546]

Johns LD, Straub SJ, Howard SM. Analysis of effective radiating area, power, intensity, and field characteristics of ultrasound transducers. Arch Phys Med Rehabil. 2007; 88:124–9. [PubMed: 17207688]

Knight MM, Roberts SR, Lee DA, Bader DL. Live cell imaging using confocal microscopy induces intracellular calcium transients and cell death. Am J Physiol Cell Physiol. 2003; 284:C1083–9. [PubMed: 12661552]

Kumon RE, Aehle M, Sabens D, Parikh P, Kourennyi D, Deng CX. Ultrasound-induced calcium oscillations and waves in Chinese hamster ovary cells in the presence of microbubbles. Biophys J. 2007; 93:L29–31. [PubMed: 17631537]

Lam KH, Hsu HS, Li Y, Lee C, Lin A, Zhou Q, Kim ES, Shung KK. Ultrahigh frequency lensless ultrasonic transducers for acoustic tweezers application. Biotechnol Bioeng. 2012

Lee J, Teh SY, Lee A, Kim HH, Lee C, Shung KK. Transverse acoustic trapping using a gaussian focused ultrasound. Ultrasound Med Biol. 2010; 36:350–5. [PubMed: 20045590]

Liu MC, Shih HC, Wu JG, Weng TW, Wu CY, Lu JC, Tung YC. Electrofluidic pressure sensor embedded microfluidic device: a study of endothelial cells under hydrostatic pressure and shear stress combinations. Lab Chip. 2013; 13:1743–53. [PubMed: 23475014]

Louw TM, Budhiraja G, Viljoen HJ, Subramanian A. Mechanotransduction of ultrasound is frequency dependent below the cavitation threshold. Ultrasound Med Biol. 2013; 39:1303–19. [PubMed: 23562015]

Mason JC, Yarwood H, Sugars K, Haskard DO. Human umbilical vein and dermal microvascular endothelial cells show heterogeneity in response to PKC activation. Am J Physiol. 1997; 273:C1233–40. [PubMed: 9357767]

Nishitani WS, Saif TA, Wang Y. Calcium signaling in live cells on elastic gels under mechanical vibration at subcellular levels. PLoS One. 2011; 6:e26181. [PubMed: 22053183]

Noriega S, Hasanova G, Subramanian A. The effect of ultrasound stimulation on the cytoskeletal organization of chondrocytes seeded in three-dimensional matrices. Cells Tissues Organs. 2013; 197:14–26. [PubMed: 22987069]

Noriega S, Mamedov T, Turner JA, Subramanian A. Intermittent applications of continuous ultrasound on the viability, proliferation, morphology, and matrix production of chondrocytes in 3D matrices. Tissue Eng. 2007; 13:611–8. [PubMed: 17518607]

Pahakis MY, Kosky JR, Dull RO, Tarbell JM. The role of endothelial glycocalyx components in mechanotransduction of fluid shear stress. Biochem Biophys Res Commun. 2007; 355:228–33. [PubMed: 17291452]

Ross D, Gaitan M, Locascio LE. Temperature measurement in microfluidic systems using a temperature-dependent fluorescent dye. Anal Chem. 2001; 73:4117–23. [PubMed: 11569800]

Shung, KK. CRC Press; Boca Raton: 2006. Diagnostic ultrasound: imaging and blood flow measurements.

Sun Z, Li Z, Meininger GA. Mechanotransduction through fibronectin-integrin focal adhesion in microvascular smooth muscle cells: is calcium essential? Am J Physiol Heart Circ Physiol. 2012; 302:H1965–73. [PubMed: 22427509]

Tanaami T, Otsuki S, Tomosada N, Kosugi Y, Shimizu M, Ishida H. High-speed 1-frame/ms scanning confocal microscope with a microlens and Nipkow disks. Appl Opt. 2002; 41:4704–8. [PubMed: 12153106]

Whitney NP, Lamb AC, Louw TM, Subramanian A. Integrin-mediated mechanotransduction pathway of low-intensity continuous ultrasound in human chondrocytes. Ultrasound Med Biol. 2012; 38:1734–43. [PubMed: 22920546]

Yamamoto K, Korenaga R, Kamiya A, Ando J. Fluid shear stress activates Ca(2+) influx into human endothelial cells via P2X4 purinoceptors. Circ Res. 2000; 87:385–91. [PubMed: 10969036]

Yoshikawa N, Ariyoshi H, Aono Y, Sakon M, Kawasaki T, Monden M. Gradients in cytoplasmic calcium concentration ([Ca2+]i) in migrating human umbilical vein endothelial cells (HUVECs) stimulated by shear-stress. Life Sci. 1999; 65:2643–51. [PubMed: 10619372]

Zhang S, Cheng J, Qin YX. Mechanobiological modulation of cytoskeleton and calcium influx in osteoblastic cells by short-term focused acoustic radiation force. PLoS One. 2012; 7:e38343. [PubMed: 22701628]

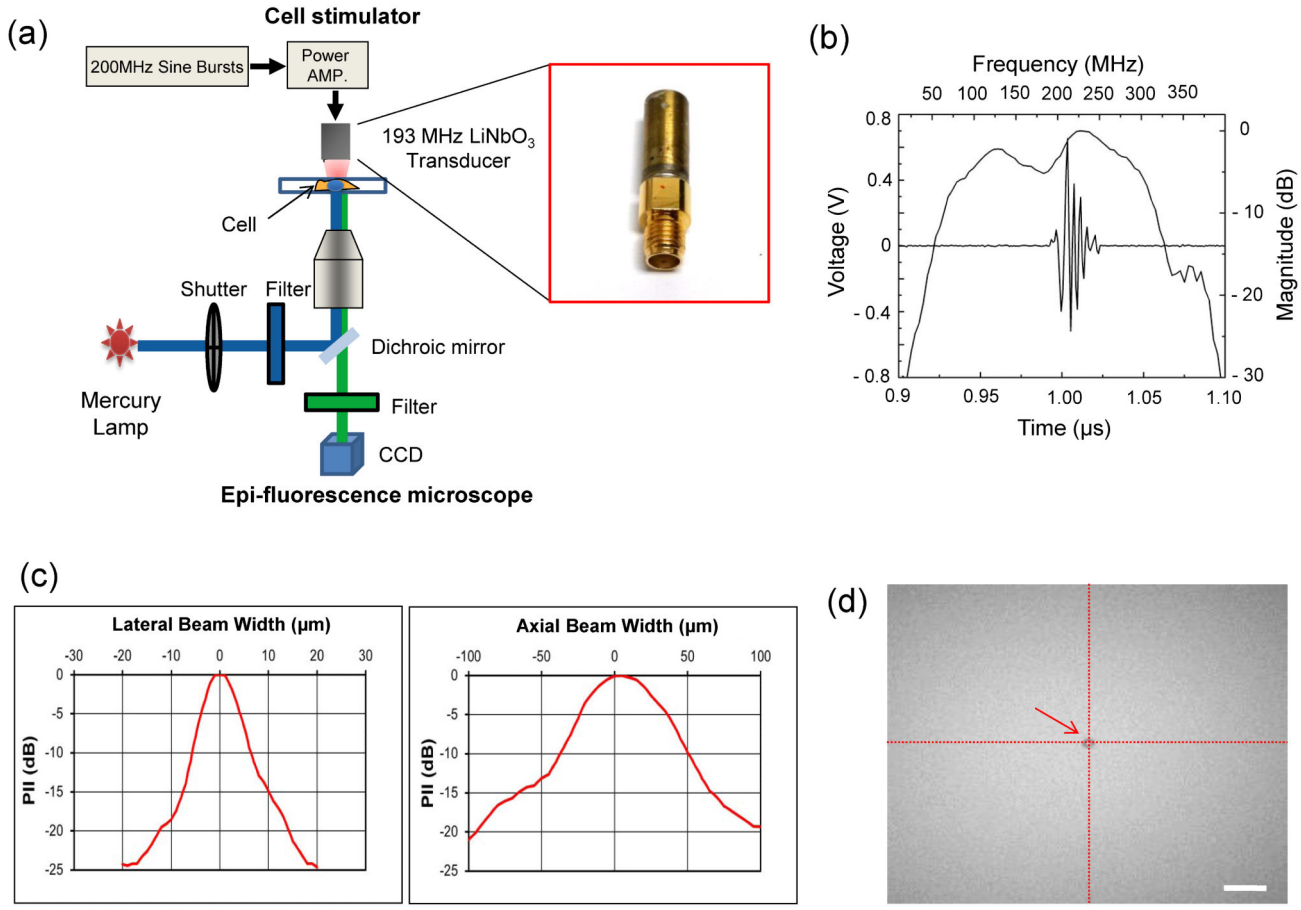

Fig. 1. Characterization of high-frequency ultrasound beams and the beam localization at the region of interest

(a) A high-frequency ultrasound mechanotransduction system (b) Pulse-echo characteristics of the transducer (c) Lateral (left) and axial (right) beam profiles. PII stands for pulse intensity integral. (d) Localization of an ultrasound microbeam at the center of an image using acoustic tweezers. The arrow indicates a 5 μm microbead trapped at beam focus. The scale bar indicates 20 μm.

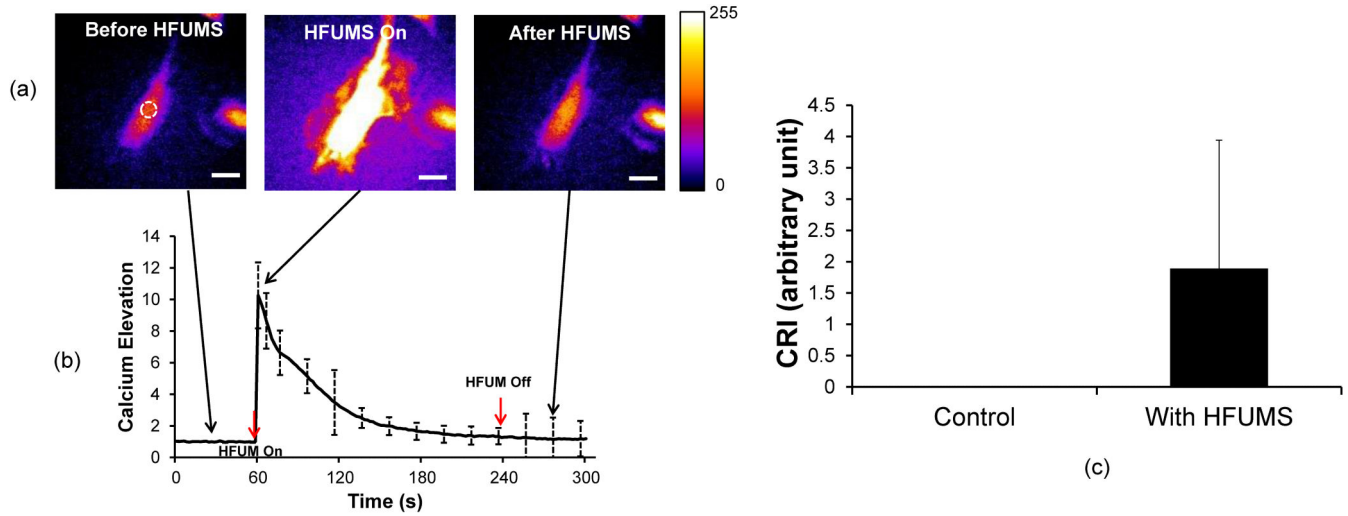

Fig. 2. Cytoplasmic Ca^{2+} changes in HUVECs due to HFUMS

(a) Fluorescence images obtained before (left), during (middle), and after (right) HFUMS (input voltage: 15.8 V_{pp}, PRF: 1 kHz, and duty cycle: 1 %) (b) Ca^{2+} changes in HUVECs over times. HFUM was switched on at 60 s and off at 240 s (c) Quantitative analysis of calcium elevation. The CRI values for HUVECs without (control) (n=21) and with (n=21) HFUMS were calculated with the program described previously. The scale bar indicates 10 μm.

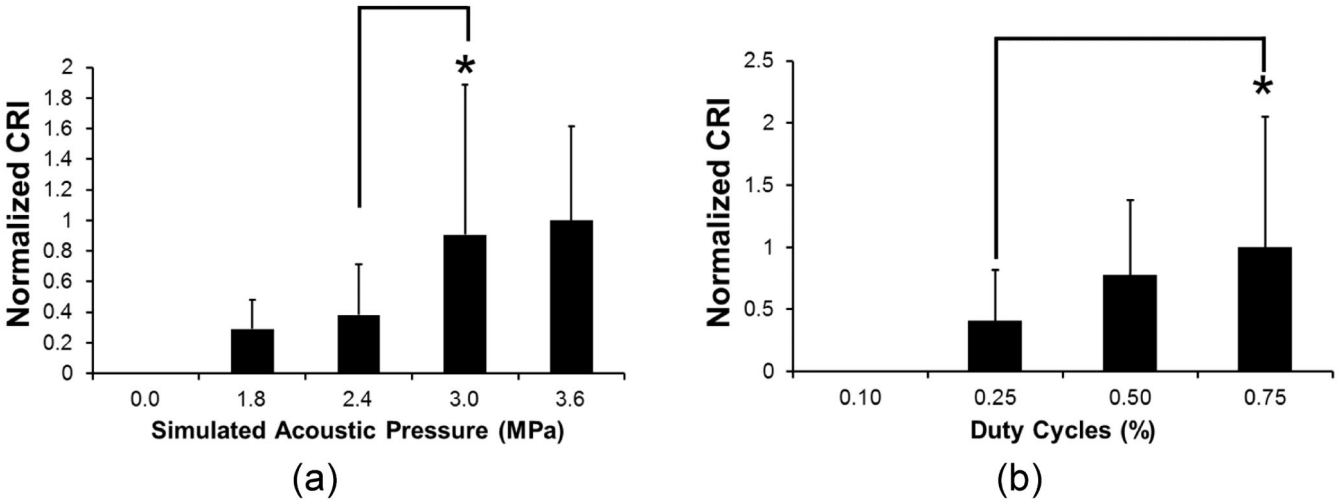

Fig. 3. Normalized CRI values for HUVECs at the simulated acoustic pressure at given input voltages (0, 9.48, 12.64, 15.80, and 18.96 V_{pp}) and duty cycles at the stimulated acoustic pressure of 3.6 MPa

(a) CRI values for HUVECs as a function of stimulated acoustic pressures at the indicated input voltages [0 MPa (n=21), 1.8 MPa (input voltage: 9.48 V_{pp}) (n=21), 2.4 MPa (input voltage: 12.64 V_{pp}) (n=21), 3.0 MPa (input voltage: 15.80 V_{pp}) (n=21), and 3.6 MPa (input voltage: 18.96 V_{pp}) (n=19)] (PRF: 1 kHz and duty cycle: 1 %). CRI values were normalized by the CRI value at 3.6 MPa (b) CRI values for HUVECs as function of duty cycles [0.1 (n=10), 0.25 (n=10), 0.50 (n=10), and 0.75 % (n=8)] [PRF: 1 kHz and simulated acoustic pressure (input voltage: 18.96 V_{pp}): 3.6 MPa (p-value: $0.25 < 0.05$)]. CRI values were normalized by the CRI value at 0.75 %.

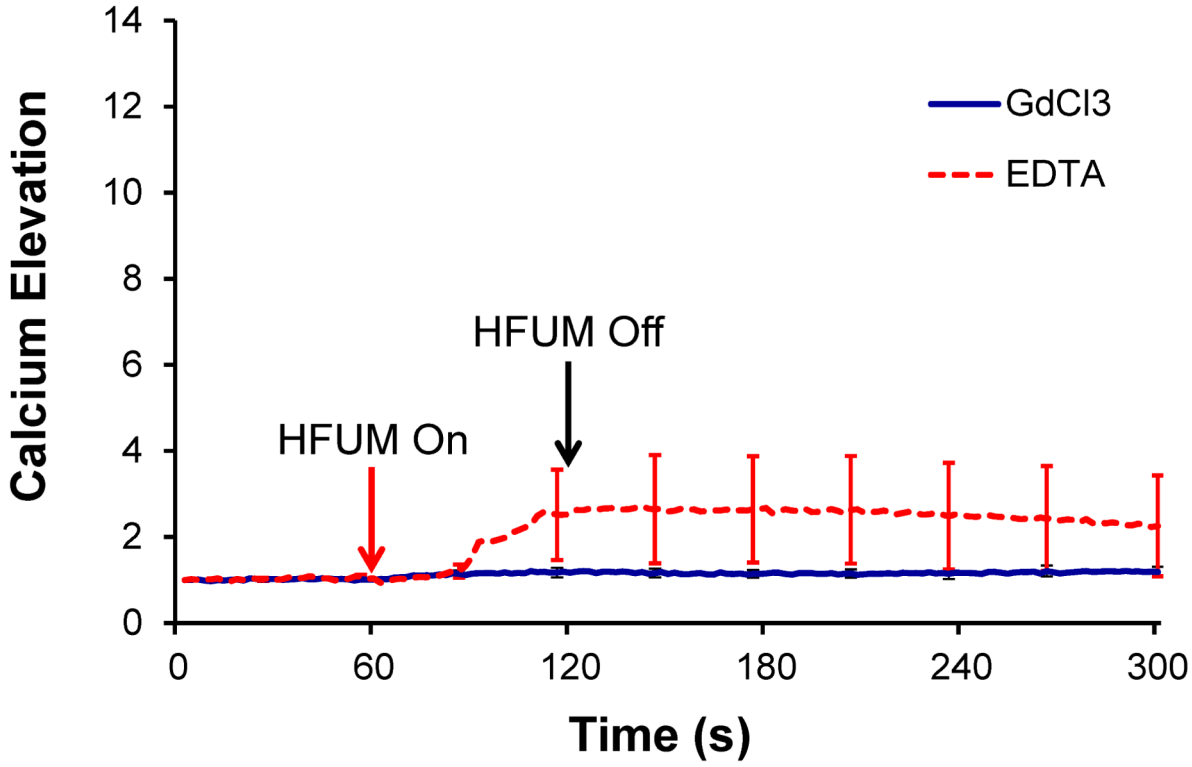

Fig. 4. Calcium elevations in HUVECs treated with Gadolinium (III) chloride ($GdCl_3$) (n=7) and EDTA (n=11) due to HFUMS

The HFUM was initiated at 60 s and off at 120 s [PRF: 1 kHz, input voltage: 18.96 V_{pp}(simulated acoustic pressure: 3.6MPa), and duty cycle: 0.5 %].

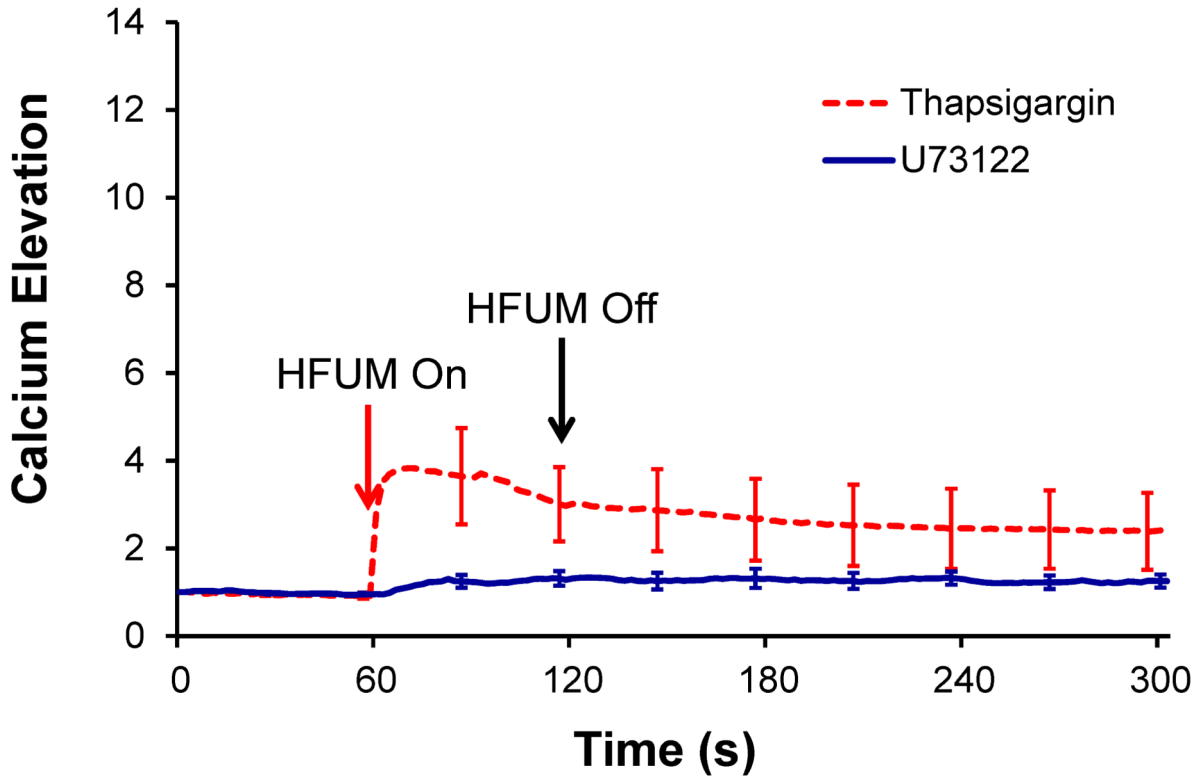

Fig. 5. Calcium elevations in HUVECs treated with ER blockers, Thapsigargin, (n=11) and PLC inhibitors, U73122 (n=11) due to HFUMS

The HFUM was initiated at 60 s and off at 120 s [PRF: 1 kHz, input voltage: 18.96 V_{pp}(simulated acoustic pressure: 3.6MPa), and duty cycle: 0.5 %]

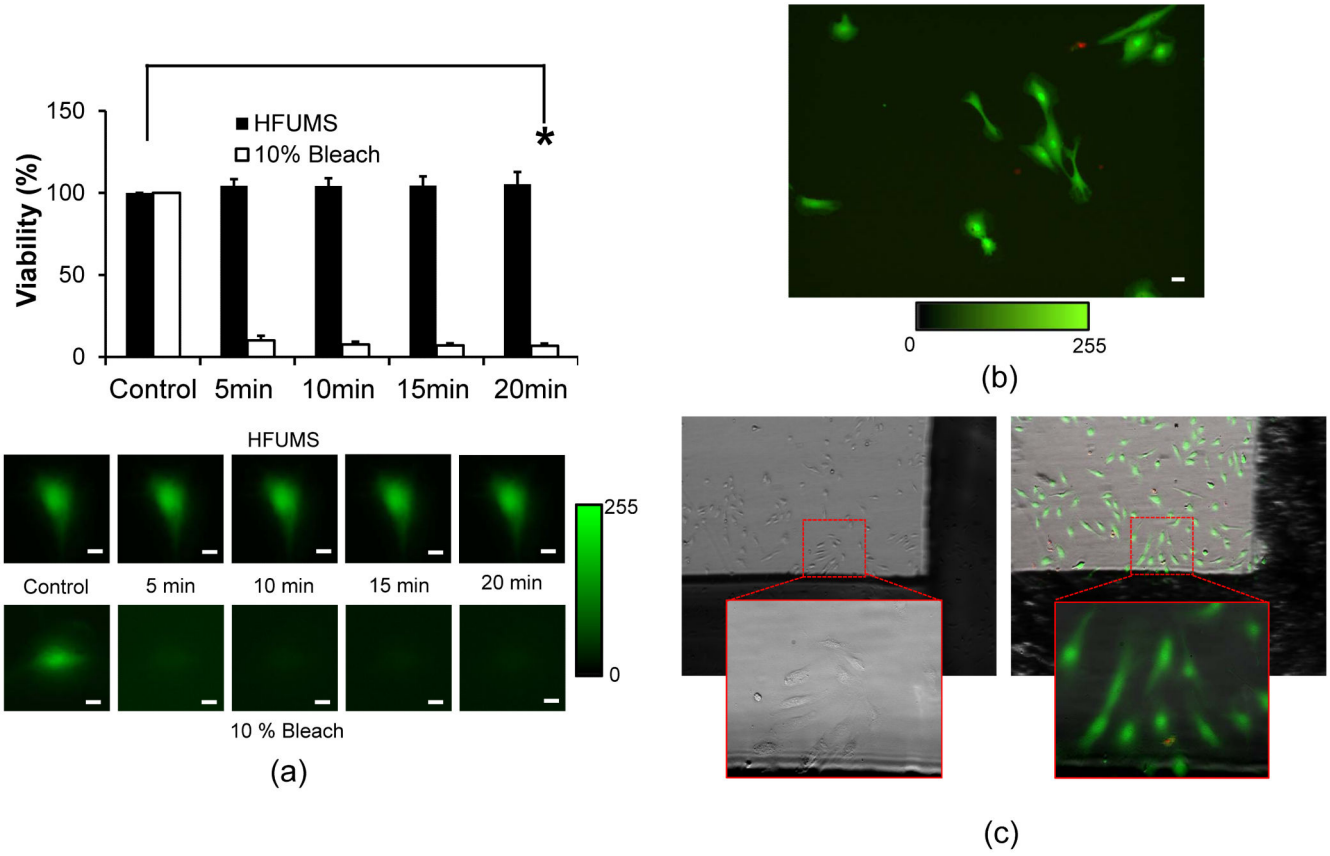

Fig. 6. Cell viability after HFUMS

(a) Cell viability changes of HUVECs at the indicated time-points (0, 5, 10, 15, 20 minutes) after HFUMS application and 10 bleach treatment (input voltage: 18.96 V_{pp}, PRF: 1 kHz, and duty cycle: 0.5 %) (n=8) and the representative fluorescence images. The viability values were normalized by the value for the viability value obtained before application of HFUM (upper) and 10% bleach treatment (lower), respectively. (b) Fluorescence images for cell viability and toxicity in 1 hours after HFUM application. The green color indicates live cells whereas the red color indicates dead cells. (c) bright-field image (left) obtained before HFUM application and overlay of a bright-field and a fluorescence image (right) for cell viability and toxicity in 24 hours after HFUM application. The dotted-red rectangular indicates the area exposed to HFUM. The solid-red rectangular represents the magnified image (20×). Scale bar: 10 μm.

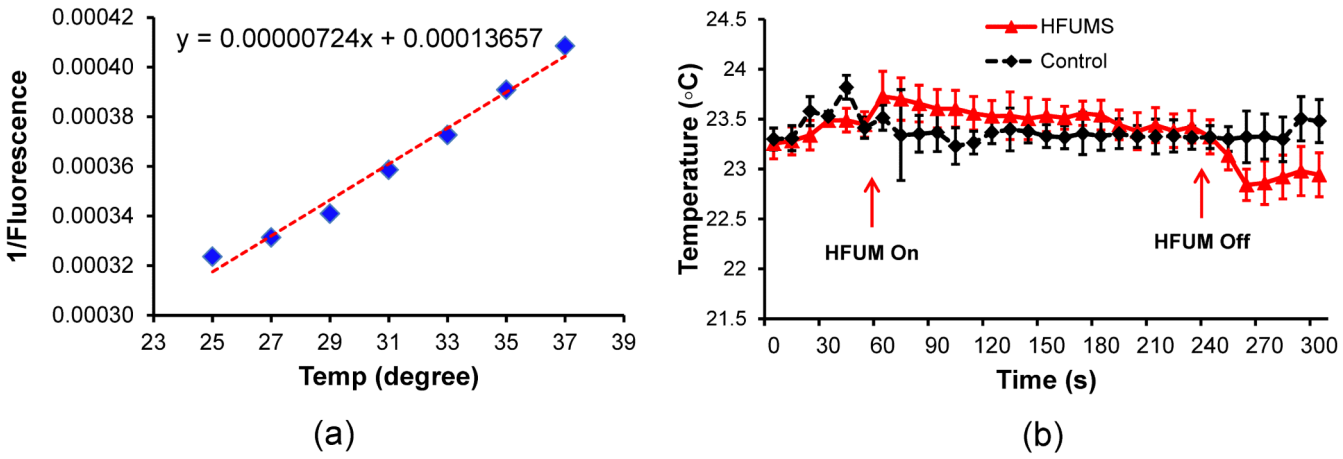

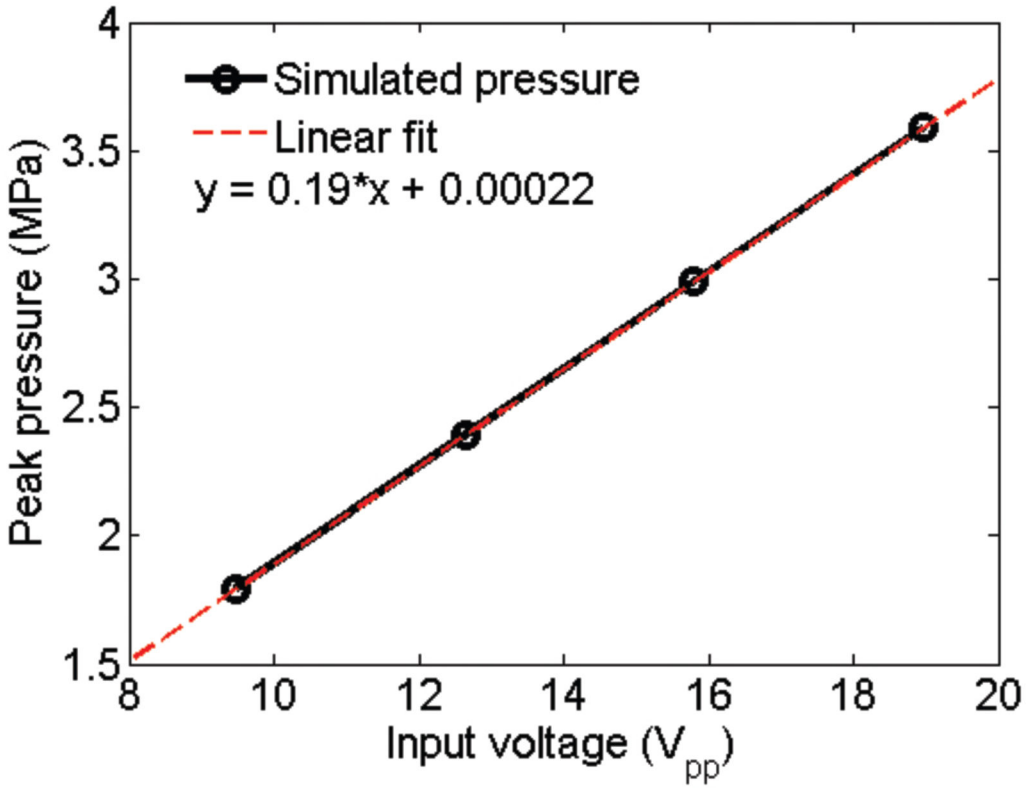

Fig. 7. HFUMS-induced temperature changes

(a) fluorescence intensity of Rhodamine B solution as a function of temperature (b) temperature changes by HFUMS. The HFUM was initiated at 60 s and off at 240 s [PRF: 1 kHz, input voltage: 18.96 V_{pp}(simulated acoustic pressure: 3.6MPa), and duty cycle: 0.5 %].